

# A Slider With an Integrated Microactuator (SLIM) for Second Stage Actuation in Hard Disc Drives

Hans H. Gatzen<sup>1</sup>, Paulo J. P. Freitas<sup>2</sup>, Ernst Obermeier<sup>3</sup>, and John Robertson<sup>4</sup>

<sup>1</sup>Leibniz Universitaet Hannover, Center for Production Technology, Institute for Microtechnology, 30823 Garbsen, Germany

<sup>2</sup>INESC MN, Microsystems and Nanotechnologies, 1000-029 Lisbon, Portugal

<sup>3</sup>Berlin University of Technology, Microsensor and Actuator Technology, 13355 Berlin, Germany

<sup>4</sup>University of Cambridge, Department of Engineering, Cambridge, CB3 0FA, U.K.

A slider with an integrated microactuator (SLIM) was devised, which is capable of actuating a read-write element of a hard disc drive (HDD) in both vertical direction (adjusting the flying height) and in lateral direction (allowing second stage actuation). The read-write element is located on a chiplet attached to a mounting platform. A pair of integrated electromagnetic microactuators appropriately activates this mounting platform and thus the read-write element. This design promises a cost competitive solution for HDD recording head microactuation. While the SLIM design as well as the thin-film fabrication of the SLIM component parts were completed, a 40 : 1 model allowed for initial system level experimental measurements which indicate a good agreement between the performance of the model and the actual SLIM device.

**Index Terms**—Electromagnetic microactuator, flying height adjustment, second stage actuation.

## I. INTRODUCTION

**P**RECONDITIONS for achieving an optimal recording density in hard disc drives (HDDs) are a minimal flying height and a perfect track registration. For accomplishing the first one, a dynamic flying height adjustment during writing and reading may optimize the head-to-disc spacing and was implemented into the latest generation of recording heads [1]. To achieve a perfect track registration, a second stage actuation is desirable to compensate the frequency limitations of the main actuator. Both flexure and microelectromechanical systems (MEMS)-based designs for second stage actuators were suggested [2], [3]. However, due to the price competitiveness of the industry, the extra costs required for such a device so far hindered its widespread use. Nevertheless, the requirements are obvious: an optimal solution will provide both capabilities for flying height and track following adjustment and will be cost competitive.

## II. SLIM CONCEPT

To address the actuator requirements, the following approach was taken: An electromagnetic microactuator was integrated into a pico form factor slider, resulting in a slider with an integrated microactuator (SLIM) [4]. Fig. 1 depicts a schematic representation of the SLIM design. Fig. 1(a) presents a diagonal rear view, while Fig. 1(b) shows a diagonal front view.

An integrated microactuator activates a mounting block to which a chiplet containing the read-write element is attached. The actuator is capable of moving the read-write element on the chiplet both in the vertical direction (adjusting the flying height) and in the lateral direction (allowing second stage actuation). The cost competitiveness results from the fact that the SLIM

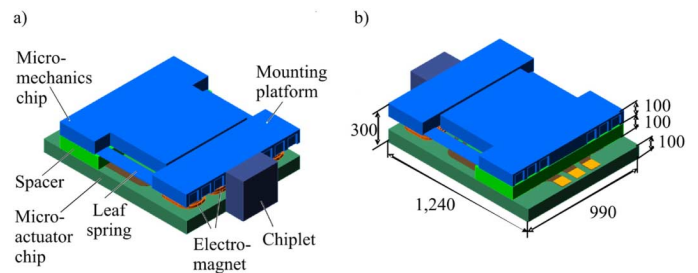


Fig. 1. Schematic representation of the SLIM. (a) Diagonal rear view; (b) diagonal front view.

components can be fabricated at lower costs than a present-day HDD slider. The microactuator is substantially less complex than a classic slider while the chiplet containing the read-write element takes up only one third of a pico slider's space.

## III. SLIM DESIGN

SLIM pursues a two-wafer approach. The actuator magnetics reside on the bottom wafer and the actuator mechanics on the top wafer. Sandwiched between the two wafers is a spacer compensating for the magnetic actuator's building height. The actuator magnetics consist of a pair of variable reluctance microactuators [5], the actuator mechanics of a mounting platform suspended by a pair of leaf springs. The mounting platform carries the chiplet containing the read-write element. Fig. 2 shows a schematic representation of the SLIM function. Simultaneously exciting both actuators adjusts the chiplet's flying height [Fig. 2(a)], while alternate excitation causes a minute rotation of the chiplet, creating a lateral displacement of the read-write element [Fig. 2(b)]. Therefore, this design allows both flying height adjustment and track following. A desired lateral displacement of  $\pm 625$  nm results in a rotation of  $0.18^\circ$ . Due to the small rotational angle, the resulting change in flying height is only about 1 nm.

Originally, the chiplet was supposed to have its own little air bearing surface (ABS). Since track following is executed through a slight rotation of the chiplet, this ABS has to have

Digital Object Identifier 10.1109/TMAG.2008.2002592

Color versions of one or more of the figures in this paper are available online at <http://ieeexplore.ieee.org>.

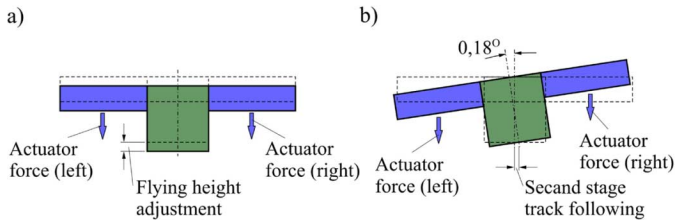


Fig. 2. SLIM actuation schematics. (a) Flying height adjustment; (b) track following.

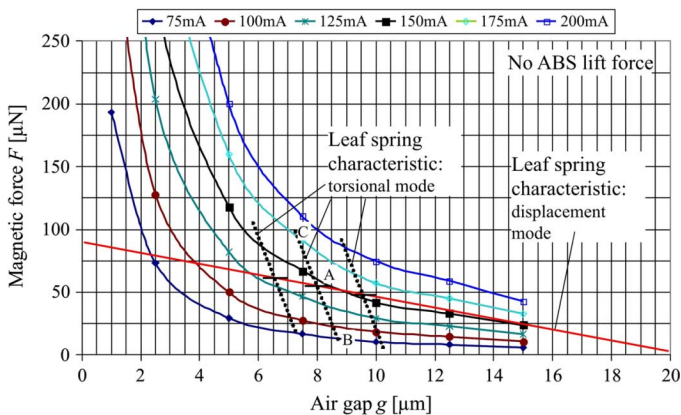


Fig. 3. System characteristics (3-D simulation).

a cross crown. ABS simulations conducted at the University of California, San Diego, showed that such an ABS has no load carrying capabilities. Therefore, ABS forces at the chiplet will be minimal.

For designing SLIM, first, an analytical model was developed, followed by modeling and simulation using the finite element method (FEM). This approach is discussed in detail in [6].

Fig. 3 presents the simulation results for the microactuator force characteristics. The parameter of curved lines represents the force curves for various excitation currents, ranging from 75 to 200 mA. The straight line with a shallow tilt represents the leaf spring characteristics in the displacement (i.e., flying height adjust) mode. The straight lines with a steep tilt represent the leaf spring characteristics for the torsional (i.e., track following) mode. Three lines are shown, representing alternative tolerance build-ups at the microactuator's air gap due to stacking tolerances and chiplet assembly tolerances.

A given excitation current results in an actuator height position represented by the respective intersection between force and spring lines. Energizing both coils with the same current results in a reduction of the air gap and thus a lowering of the chiplet to its desired flying height (operating point A). For the track following, the torsional contributions of the leaf springs dictate the actuator behavior. By reducing the current in one coil (operating point B) while increasing it by approximately the same amount in the other coil (operating point C), a tilting motion required for a lateral track adjustment is accomplished.

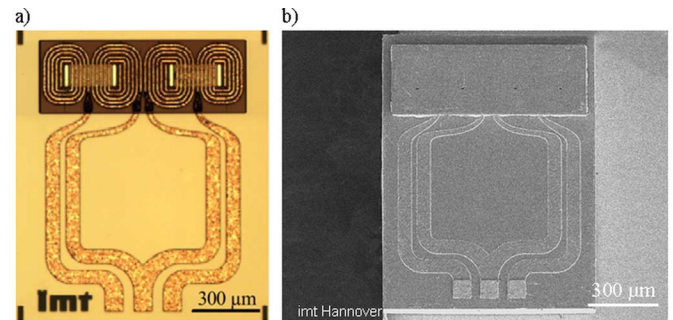


Fig. 4. SLIM micromagnetics. (a) Optical micrograph of the first coil layer; (b) SEM micrograph of the completed SLIM micromagnetics.

It is desirable to get an experimental verification of the simulation results before the availability of functional thin-film devices. To do so, a scaled-up device was both fabricated and subjected to FEM simulations. Comparing these results and extrapolating them allows us to predict the behavior of the real size device.

#### IV. FABRICATION

An SLIM device consists of three chips stacked on top of each other [Fig. 1(a)]: a bottom chip contains the actuator magnetics, a top chip the actuator mechanics, and a spacer serves to join both. For assembling the slider body, the top chip, the bottom chip, and the spacer will be bonded to each other.

##### A. Micromagnetics Fabrication

The micromagnetics fabrication was executed on a 525- $\mu\text{m}$ -thick Si wafer with a diameter of 100 mm serving as a substrate. Ultimately, the wafer has to be thinned to the desired device height of 100  $\mu\text{m}$ . Since the energy a microactuator converts is proportional to its volume, a high aspect ratio microstructure technology was applied [5], [7].

The first fabrication step was the plasma-enhanced chemical vapor deposition of an  $\text{Si}_3\text{N}_4$  insulation layer. Then, the bottom flux guide was fabricated. This process started with sputter depositing an Au seed layer, followed by creating a photoresist micromold. An electroplating process created the NiFe45/55 flux guide. After stripping the micromold for the flux guide, another micromold was created. It served for the deposition of the electric leads and vias. Next, the flux guide and leads were embedded in SU-8<sup>1</sup> and planarized using chemical-mechanical polishing. A reinforcement at the leading edge created the contact pads. The seed layer was removed after stripping the photomask to avoid shorts between the coil turns. A coat of low stress  $\text{Si}_3\text{N}_4$  formed an insulation layer.

For the second coil and core layers, the same fabrication sequence was applied. As a result, actuators with NiFe45/55 C-cores and dual layer Cu spiral coils were fabricated. A detailed description of the fabrication is provided in a separate article in this issue [5]. Fig. 4(a) depicts the SLIM micromagnetics after finishing the second coil layer, Fig. 4(b) an SEM micrograph of the completed system.

<sup>1</sup>Trademark.

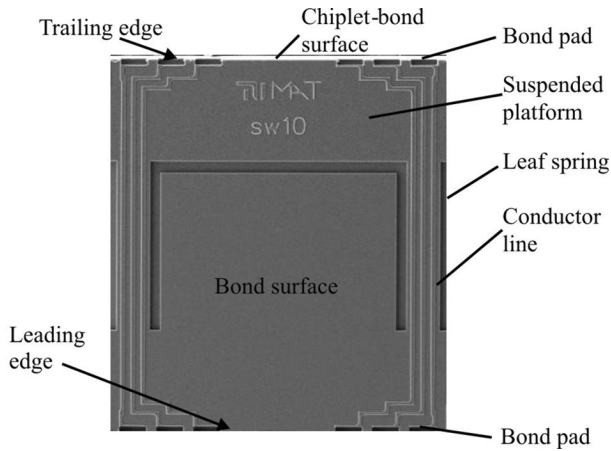


Fig. 5. Completed SLIM micromechanics.

### B. Micromechanics Fabrication

The micromagnetics fabrication was executed on a 300- $\mu\text{m}$ -thick silicon-on-insulator (SOI) wafer of 100 mm diameter. It consists of a sandwich of a 100- $\mu\text{m}$ -thick device wafer and a 200- $\mu\text{m}$ -thick handling wafer, separated by an  $\text{SiO}_2$  layer. The first step was to deposit a NiFe 45/55 flux guide by electroplating. In the next step, the cavities were etched which ultimately are forming the leading and trailing edge contacts for connecting the read-write element on the chiplet. Next, the contact pads and leads were metallized. This concluded the fabrication processes on this wafer surface. Fig. 5 shows the results.

The remaining fabrication steps were done on the backside of the device wafer. Before they could be executed, the SOI wafer had to be thinned down to the device wafer thickness. This was done by a combination of cupwheel grinding and deep reactive ion etching. Since the thinned device wafer had a thickness of only 100  $\mu\text{m}$ , it was bonded to a new handling wafer. Next, the remaining fabrication steps on the wafer topside were executed, creating the notch for releasing the mounting block and releasing the leaf springs. Releasing the device wafer from the handling wafer concluded the wafer fabrication process for the SLIM micromechanics. At this point in time, all components were completed and are awaiting system integration.

### C. Slider Body Assembly

As discussed before, to form the SLIM body, three components have to be stacked: a bottom part containing the micromagnetics, a top part containing the micromechanics, and a spacer to keep both parts at the desired distance.

Fig. 6 gives a schematic representation of the integration concept for forming the SLIM bodies, which is executed on a row bar level. A row bar contains two rows with ten sliders each facing each other. On either end of the rows, an anchor firmly supporting the mounting platforms is integrated in the micromechanics. This way, the leaf springs ultimately suspending the mounting platforms are not yet released and will stay that way until the row bars will be separated to form the slider bodies. An-

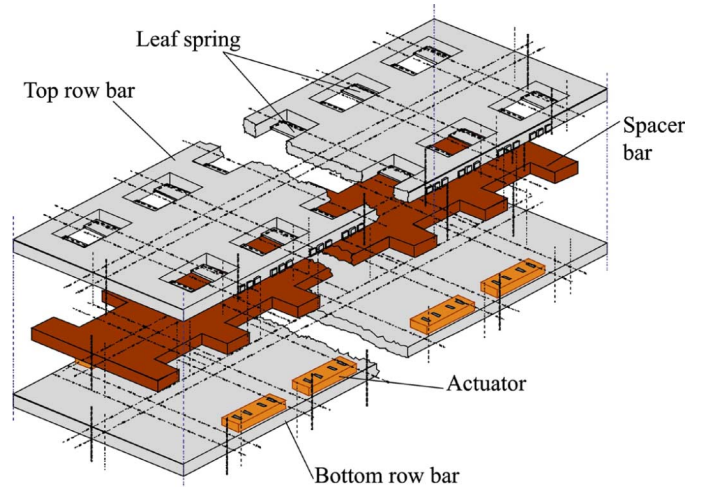


Fig. 6. Bar level slider body assembly.

choring the mounting platform will also make it easier to mount the chiplet.

While all component parts are available, the stacking process itself is still under development. This is the main reason a scaled-up model was built.

Ultimately, on the wafer's backside, an ABS will be created by ion milling and covered by a DLC layer. However, for the first prototypes, this ABS will not be included, since the initial testing will be performed on a static tester.

Due to the fact that the slider body consists of Si, increasing the wear resistance is mandatory. While a great hardness of the DLC film is desirable, excessive film stress is prohibitive. For finding an optimum, Raman spectroscopy is applied as an analysis tool [8]. For coating the slider body ABS, a DLC film thickness of 50 nm was chosen. Due to head-to-disc spacing limitations, a much thinner DLC film has to be chosen for the chiplet. The film thickness will be 1 to 2 nm and mainly serves as a corrosion protection.

## V. EXPERIMENTAL INVESTIGATIONS

### A. Investigations on a Scaled-up Model

To allow for early experimental investigations of the mechanical behavior of SLIM, a functional 40 : 1 scale model of SLIM was created. By considering scaling laws and comparing simulation results for the actual SLIM device and the large-scale model, initial experimental data could be gained.

Scaling is governed by the following equation:

$$F_m = \frac{N^2 I^2}{\mu_0 A_g (\sum R_{mi})^2} \quad (1)$$

with  $F_m$  the magnetic force,  $N$  the number of turns,  $I$  the current,  $\mu_0$  the magnetic constant,  $A_g$  the gap area, and  $R_{mi}$  the reluctance. Comparing the real-size and the large-scale models, the number of turns is the same, the currents differ, the reluctance ratio  $R_{skal}/R_{real}$  is 0.02, and the air gap area scales by  $40 \times 40$ .

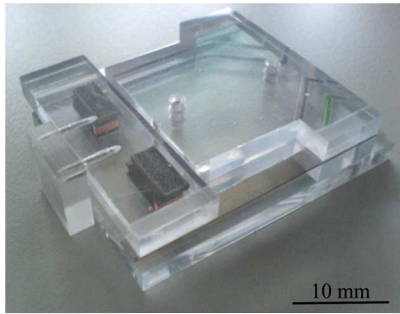


Fig. 7. Scaled-up SLIM model.

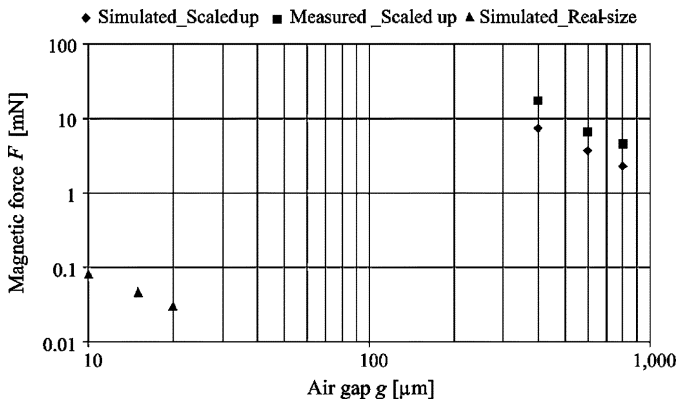


Fig. 8. Comparison between theoretical and experimental results.

Fig. 7 depicts the scaled-up model. For conducting the experiments, a test stand was created. It allows us to adjust the actuator's air gap and to measure the actuator force exerted on the chiplet as a function of the excitation current and the air gap length.

Fig. 8 compares theoretical and experimental results for the actuator forces, showing simulation results for the real-size SLIM as well as the scaled-up SLIM and experimental data for the large-scale SLIM. The measured force slightly exceeds the simulated force for the large-scale model. This allows the assumption that the modelling results for the real-size SLIM are within the expected range.

### B. Pole Field Measurements

A direct way to judge the magnetic capabilities of the real-size SLIM on a micromagnetics level is to measure the magnetic field the poles are capable of creating with no flux closures present (i.e., measurements against air) and comparing it to respective simulation results. Measurements conducted jointly by the Universities of Colorado in Colorado Springs and the Colorado State University in Fort Collins showed a good match with the simulations against air. The results are described in detail in [6].

## VI. CONCLUSION AND OUTLOOK

The work performed so far indicates that the SLIM concept may provide a cost competitive approach not only to RDD second stage actuation, but also to flying height adjustment. By choosing a two-wafer design, a path towards a separate fabrication of the micromagnetics (executed on a bottom wafer) and micromechanics (executed on a top wafer) could be found and was verified by executing respective fabrication steps. Experimental investigations with a scaled-up model proved the feasibility of the concept.

In a next step, the SLIM device will be mounted to a flexure and subjected to stationary tests on an aerostatic test fixture. For monitoring the chiplet's lateral motion, the displacement of a permanent micromagnet deposited on the chiplet will be monitored by a GMR array. A major challenge will be to come up with a chiplet attachment process yielding a maximal air gap tolerance of  $\pm 0.75 \mu\text{m}$  and maintaining tight angular tolerances. Ultimately, the SLIM head gimbal assembly will be subjected to spin-stand tests.

### ACKNOWLEDGMENT

This work was sponsored in part by the European Commission within the Framework 6 Information Society Technologies Programme's Specific Target Research Project (STREP) PARMA (Performance Advances in Recording through Micro Actuation). Furthermore, the authors would like to thank Seagate Technology LLP for supporting the program, among others through donating test equipment and F. E. Talke, University of California, San Diego, for conducting ABS simulations.

### REFERENCES

- [1] D. W. Meyer, P. E. Kupinski, and J. C. Liu, "Slider With Temperature Responsive Transducer Positioning," U.S. Patent 5991113.
- [2] L.-S. Fan, H. H. Ottesen, T. C. Reiley, and R. W. Wood, "Magnetic recording head positioning at very high track densities using a microactuator-based, two-stage servo system," *IEEE Trans. Ind. Electron.*, vol. 42, no. 3, pp. 222–233, 1995.
- [3] Y. Lu, J. P. Yang, J. Chen, and S. X. Chen, "A silicon microactuator-integrated microfabrication technology," *IEEE Trans. Magn.*, vol. 39, no. 5, pt. 2, pp. 2240–2242, Sep. 2003.
- [4] H. H. Gatzen, "Schreib-/Lesekopf Mit Integriertem Mikroaktor (Read-Write Head With Integrated Micro Actuator)," German Patent 10260009.
- [5] D. Dinulovic, H. Saalfeld, Z. Celinski, S. Field, and H. H. Gatzen, "Integrated electromagnetic second stage micro actuator for a hard disc recording head," in *Intermag Madrid*, 2008, accepted for publication.
- [6] D. Dinulovic and H. H. Gatzen, "An approach for simulating magnetic microactuators," in *Proc. EuroSimE*, Freiburg, Germany, 2008, pp. 217–220.
- [7] C. Ruffert and H. H. Gatzen, "Fabrication and test of multi layer micro coils with a high packaging density," in *HARMST2007*, Besançon, France, 2007, pp. 245–246, Book of Abstracts.
- [8] C. Casiraghi, A. C. Ferrari, and J. Robertson, "Raman spectroscopy of hydrogenated amorphous carbon," *Phys. Rev. B*, vol. 72, p. 085401, 2005.

Manuscript received March 03, 2008. Current version published December 17, 2008. Corresponding author: H. H. Gatzen (e-mail: gatzen@imt.uni-hannover.de).